Laser direct metal deposition process of thin-walled parts using variable spot by inside-beam powder feeding

Lifang Wang
Engineering Training Center, Soochow University, Suzhou, China
Gangxian Zhu, Tuo Shi, Jizhuo Wu, Bin Lu and Geyan Fu
School of Mechanical and Electrical Engineering, Soochow University, Suzhou, China, and
Yunxia Ye
School of Mechanical Engineering, Jiangsu University, Zhenjiang, China

Abstract

Purpose – The purpose of this paper is to improve the forming efficiency and quality of unequal-width parts fabricated by laser direct metal deposition technology, some experiments were designed.

Design/methodology/approach – A new method by varying laser spot was adopted to fabricate unequal-width single track using one scanning rather than multi-track overlapping in the way of the inside-beam powder feeding, and the thin-walled parts were fabricated layer by layer. The theoretical model among layer thickness of *z*-axis, height of single track and the section curve order of single track was established.

Findings – The top surface unevenness of the thin-walled parts could be compensated automatically within the laser defocusing ranges from −2.5 to −5 mm and from 0.5 to 2.5 mm. The growth rate with the large width/height ratio was more than the small ratio, while the set height of the single track was uniform. The problem of non-uniform growth rate could be solved based on a stepped single-track method. The thin-walled parts with the smooth top surface was fabricated layer by layer which had a continuously variable width from 1 to 3 mm by splicing the laser defocusing range.

Practical implications – The shapes of the to-be-fabricated parts affect variable laser spot process in practical applications. For example, it will be difficult to apply variable laser spot process on the parts with the hole features.

Originality/value – This paper provided a guidance for forming unequal-width parts by laser direct metal deposition based on the inside-beam powder feeding.

Keywords Inside-beam powder feeding, Laser direct metal deposition, Self-regulation effect, Unequal-width thin-walled part, Variable laser spot

Paper type Research paper

Downloaded by 121.228.30.1 At 15:16 08 February 2018 (PT)

1. Introduction

The large thin-walled parts with variable width have been widely applied in aviation, aerospace and some high-technology fields. These kinds of parts are characterized as complicated technological process, thinner width and complex structures. These characteristics make the traditional manufacturing technologies face great challenges (Dinda *et al.*, 2009; Li *et al.*, 2013; Wang, 2014). As one of the most promising additive manufacturing technologies, laser direct metal deposition (LDMD) technology can be used to directly build three-dimensional fully dense metal components with excellent mechanical properties, and therefore, it has been recognized as a promising application foreground in aerospace, automotive, ships and weapon equipment fields (Mazumder *et al.*, 2000; Gu *et al.*, 2012; Dutta *et al.*, 2009).

At present, the thin-walled parts with variable width are fabricated by multi-track overlapping way in LDMD technology. There are two aspects of shortcomings. On the one hand, the surface roughness is strongly dependent on the overlapping ratio, and the unreasonable overlapping ratio will directly cause the incline of the cladding layer surface. Once this happens, the forming quality of cladding layer will be difficult to control, which will force the forming process to cease (Pi *et al.*, 2011; Cao *et al.*, 2013). On the other hand, the forming efficiency is low (Wu, 2007).

To improve the forming efficiency and quality of current LDMD technology, a new method by varying laser spot was put forward to fabricate the unequal-width single track using one scanning rather than multi-track overlapping, and the thin-walled parts were fabricated layer by layer. Figure 1 shows the

The current issue and full text archive of this journal is available on Emerald Insight at: **www.emeraldinsight.com/1355-2546.htm**

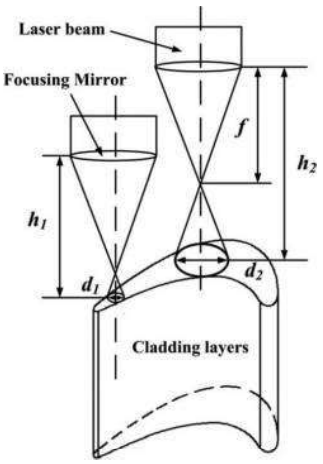


Rapid Prototyping Journal
24/1 (2018) 18–27
© Emerald Publishing Limited [ISSN 1355-2546]
[DOI 10.1108/RPJ-01-2016-0010]

The work was financially supported by the National Natural Science Foundation of China through Grant No. 51405319, 61475107, the National Key Research Program of China through Grant No. 2016YFB1100300 and the Sci-Tech Plan Project of Suzhou municipal of China through Grant No. SYG201643.

Received 22 January 2016
Revised 25 October 2016
28 December 2016
Accepted 17 January 2017

Figure 1 Principle of LDMD with varying laser spot



manufacturing principle of the new method. In view of varying laser spot in DMD technology, little research work was carried out. The German Reis Machinery Manufacturing Company cooperating with Fraunhofer Institute for Laser Technology reported that a variable focal length nozzle had been developed, but the forming process had not been declared (Peis REIS LASERTEC, 2011). In addition, to actually realize the coupling of coaxial laser beam and powder and improve the powder utilization efficiency, a specially designed coaxial nozzle was used to transfer the external-side powder feeding to inside-beam powder feeding.

In this paper, the forming process of thin-walled parts with variable width was studied using varying laser spot process, the effect between laser defocusing distances under the conditions of continuous and piecewise continuous changes and the forming quality of thin-walled parts was analyzed in detail, and the forming quality of thin-walled parts was also investigated with uniform and stepped cladding height during deposition based on inside-beam powder feeding method.

2. Experimental procedure

The experiments were carried out with the setup shown in Figure 2. The system included a fiber laser with 2 KW maximum output power, a six-axis robot, a two-axis NC tilting worktable and a powder feeding system. The powder feeding system consisted of

Figure 2 Schematic diagram of the experimental setup



a powder feeder and a specially designed coaxial nozzle, which made the laser beam be split by a cone mirror and then focused by another ring mirror. Subsequently, the parallel beam was transferred into an internal hollow beam. By this method, the way of external-side powder feeding was transferred to inside-beam powder feeding, as shown in Figure 3 (Shi *et al.*, 2006). The laser beam was guided to the worktable through an optical fiber and focused by an optical system with a 192 mm focal length. The powder used was Fe-based 313. The compositions of the powder are shown in Table I. The diameters range of the particles were 45-74 μm. The substrate material used in experiments was stainless steel 304 with a size of 150 × 100 × 10 mm, and its chemical compositions are shown in Table II.

First of all, the good quality single track was acquired by optimizing, the basic process parameters as laser power of 600 W, powder mass flow rate of 8 g/min, laser defocusing distance of −1 mm and scanning speed of 14 mm/s through preliminary experiments. A schematic diagram for typical single track is illustrated in Figure 4(a).

Second, different widths of single tracks with the uniform height were obtained, and the corresponding process parameters had also been gotten by adjusting the laser power

Figure 3 Schematic diagram of nozzle with inside-beam powder feeding

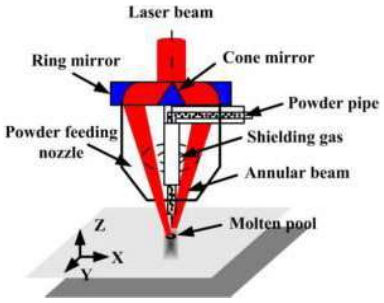


Table I Compositions of the Fe-base 313 powder

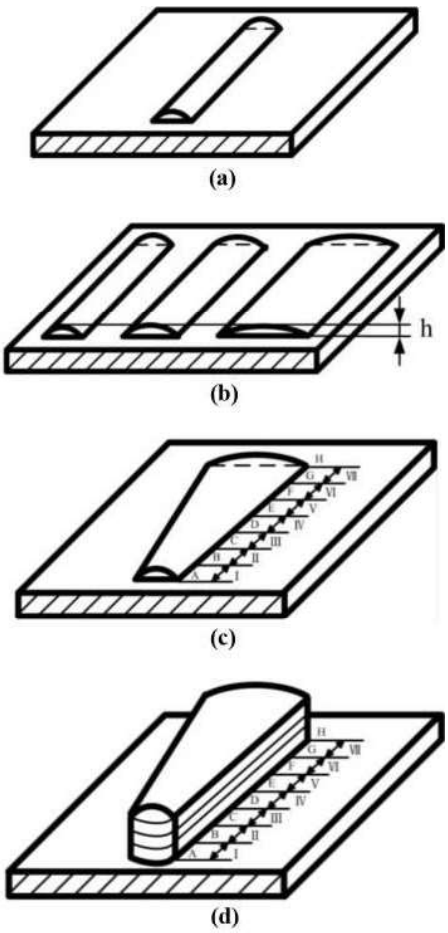
Element	Wt.%
C	0.1
Si	2.5-3.5
Cr	13-17
B	0.5-1.5
Fe	Base

Table II Compositions of the stainless steel 304 substrate

Element	Wt.%
C	0.08
Si	0.96
Mn	1.85
P	0.029
S	0.027
Cr	17.31
Ni	8.01
Fe	Base

Downloaded by 121.228.30.1 At 15:16 08 February 2018 (PT)

Figure 4 The flow chart of experimental procedure



Notes: (a) The Step 1; (b) the Step 2;(c) the Step 3; (d) the Step 4

and scanning speed with different laser defocusing distances. The process is shown in Figure 4(b).

Third, an unequal-width single track with the uniform height was gained. A geometrical model was built, and its width gradually changed from 1 to 3 mm with a constant height. The length of single track was 80 mm, as shown in Figure 4(c). The laser defocusing range was from −5 to 5 mm because of the nozzle structure limitation. The negative defocusing range from −5 to 0 mm was divided into seven sections which were marked as 1 to 7 in the experiments. The laser defocusing distance of the start Section 1 was constant at 0 mm, while the end Section 7 was −5 mm, respectively. The laser defocusing distances from Sections2 to 6 were gradually changing from 0 to −5 mm. The specific process parameters of each section are shown in Table III according to the experimental results from the Step 2. In addition, every section was further divided into ten portions so that the process parameters continuous changing was realized. Meanwhile, every portion had a definite laser power, laser defocusing distance and scanning speed value. For example, in Section 2, the laser defocusing distance changed every 0.1 mm from 0 to 1 mm, laser power changed every 20 W from 200 to 400 W and scanning speed changed every 0.4 mm/s from 10 to 14 mm/s. That is to say, the continuously changed process parameters were approximately realized by discrete stepped splicing in this research. Finally, the thin-walled parts were fabricated layer by layer based on the Step 3 process, as depicted in Figure 4(d). By the way, the part was cut by the electric discharge wire cutting machine perpendicularly along the scanning direction. After being carefully grinded and polished, the heights and widths of the cross sections and the microstructures were checked by optical microscope (Model Leica DM-IRM, Germany).

Table III The corresponding process parameters of each segment

Cross-section	Laser defocusing distance/(mm)	Laser power/(W)	Scanning speed/(mm/s)
I (A→B)	0	400	10
II (B→C)	0 → −1	400 → 600	10 → 14
III (C→D)	−1 → −2	600 → 800	14 → 15
IV (D→E)	−2 → −3	800 → 1,000	15
V (E→F)	−3 → −4	1,000 → 900	15 → 11
VI (F→G)	−4 → −5	900 → 1,000	11 → 10
VII (G→H)	−5	1,000	10

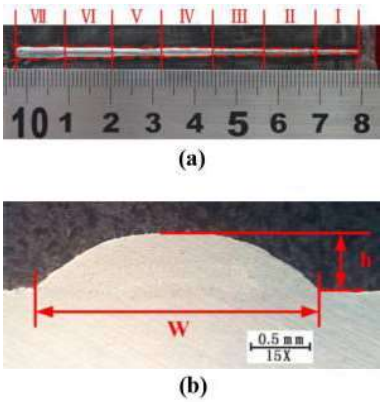
3. Results and discussion

3.1 Unequal-width single tracks fabricated using variable laser spot process

Using the process parameters that are listed in Table III, the single-track experiments were conducted by variable laser spot process. The deposited single track and section profile of cladding layer are shown in Figure 5. The measured widths and heights and the corresponding process parameters are shown at B, C, D, E, F, G positions in Table IV, respectively.

It is observed from Figure 5 and Table IV that an unequal-width single track with uniform height was realized by controlling scanning speed and laser power with different laser defocusing distances.

Figure 5 The unequal-width single tracks and its section profile



Notes: (a) The single track; (b) section profile of cladding layer

Downloaded by 121.228.30.1 At 15:16 08 February 2018 (PT)

Table IV The corresponding process parameters and section sizes of single tracks

Position	Laser power/(W)	Scanning speed/(mm/s)	Width/(mm)	Height/(mm)
B	400	10	1.06	0.50
C	600	14	1.36	0.48
D	800	15	1.46	0.49
E	1,000	15	1.53	0.46
F	900	11	1.90	0.47
G	1,000	10	2.43	0.49

In fact, the determinant factors which influenced molten pool size were laser beam energy and powder amount injected into molten pool. The energy absorbed by molten pool was computed by laser energy density E_l($E_l = P/D_lV$, P-laser power, D_l-laser spot diameter, V-scanning speed), and the powder amount injected into molten pool was calculated by powder mass density E_p ($E_p = M_P/D_pV$, M_P-powder mass flow rate, D_p-powder convergent diameter, V-scanning speed).
According to the linear optics and geometry calculation, the laser spot size $d(z)$ was given in terms of the laser defocusing distance, whose functional expression was followed in Formula (1). Then, the outside diameter of the laser spot size was calculated with the different laser defocusing distances, respectively, as shown in Table V:

$$d(z) = d_0 + \frac{D - d_0}{f_l}|z| \quad (1)$$

where f_l was the focal length of the objective lens, d_0 was the laser spot size after focusing, D was the raw beam spot size before focusing and z was the laser defocusing distance.

The powder convergent characteristics were photographed by a MicroPublisher 5 RTV high speed camera from Canadian Qimaging Corporation, as shown in Figure 6. It was seen that the powder convergent characteristic was good at about 2 mm.

Then, the laser energy density and powder mass density are computed according to Tables IV and V at positions of B, C, D, E, F, G, respectively. The results are shown in Table VI.
As being observed from Table VI, the laser energy density was steady at about 33 J/mm^2, and powder mass density was stable at about 5×10^{-3} g/mm^2. So, the objective of requiring an unequal-width single track with uniform height came true by using variable spot process while keeping the laser mass density and powder mass density constant.

Table V Laser outside spot sizes with different laser defocusing distances

Laser defocusing distance/Z (mm)	Laser outside spot size/D(mm)
0	1.00
±1	1.38
±2	1.76
±2.5	1.95
±3	2.13
±4	2.51
±5	2.89

Figure 6 The powder convergent characteristics

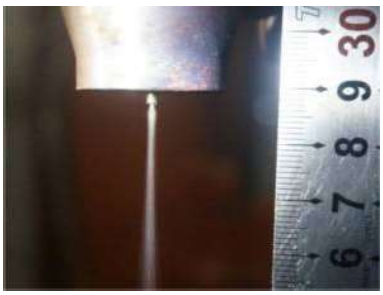


Table VI The laser energy density and the powder mass density calculated

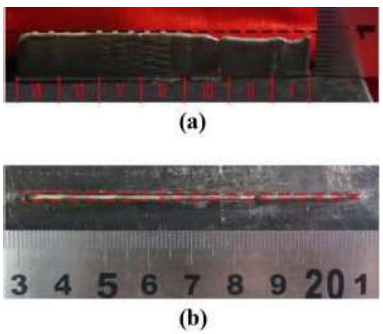
Position	Laser energy density/(J/mm^2)	Powder mass density/10^{-3}(g/mm^2)
B	40.00	6.67
C	31.06	4.76
D	30.30	4.44
E	31.30	4.44
F	32.60	6.06
G	34.60	6.67

3.2 Thin wall fabricated layer by layer using variable laser spot

In the experiment, the z-axis increment was equal to 2/3 h (here, h standed for the section height of single track) according to the z-axis increment model from reference (Zhu, 2011), so the smooth surface of the cladding layers was obtained. The thin wall was built using varying laser spot process layer-by-layer deposition with the process parameters listed in Table III. The layer number of the thin wall was 25, and the total building height was 8.5 mm. The fabricated thin-walled sample is shown in Figure 7.

As shown in Figure 7, the top surface was smooth with the laser defocusing range from −3 to −5 mm (V-VII segments). But the top surface was uneven with the laser defocusing range from 0 to −2 mm (I-III segments). According to references (Pinkerton and Li, 2004; Li *et al.*, 2007), it was predicted that the unevenness of the thin-walled parts top surface could be

Figure 7 A thin-walled sample



(a)

(b)

Notes: (a) The front view; (b) the top view

Downloaded by 121.228.30.1 At 15:16 08 February 2018 (PT)

Downloaded by 121.228.30.1 At 15:16 08 February 2018 (PT)

compensated automatically by the consequent successive layers with the laser defocusing range from −3 to −5 mm, which was also called self-regulation effect. However, this effect could not be achieved within the laser defocusing distance range from 0 to −2 mm.

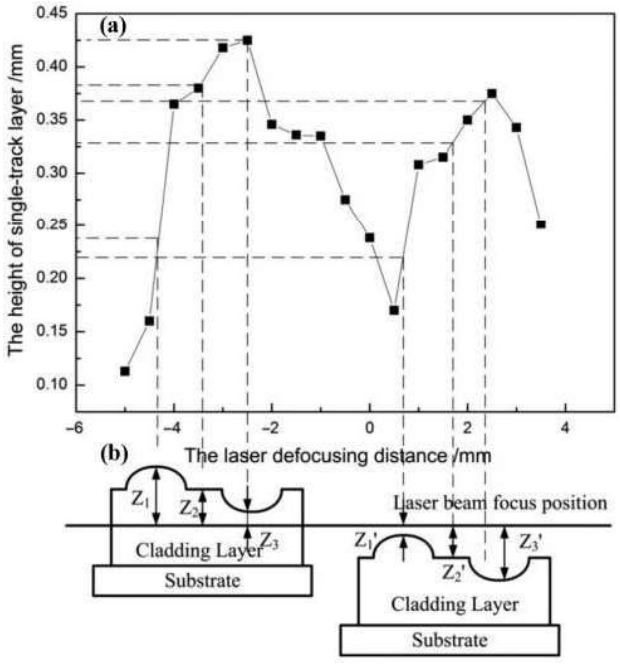
The single-track experiments were designed to acquire the relationship between the height of single track and laser defocusing distances and verify the self-regulation effect prediction and try to find the reasonable laser defocusing distances. The process parameters adopted are listed in Table VII, and the experimental results are measured and shown in Figure 8(a).

It can be seen from Figure 8(a), the height of cladding layer first increased and then decreased with the growth of laser defocusing distance varying from −5 to 0 mm, which was the negative defocusing range, and the maximum height value appeared at the defocus distance of −2.5 mm. Within the positive defocusing range from 0 to 4 mm, the varying rule of the cladding layer height was similar to that of laser negative defocusing range, while the peak height value showed at 2.5 mm.

Table VII Process parameters in single-track cladding

Laser defocusing distance/(mm)	Powder mass flow rate/(g/min)	Laser power/(W)	Scanning speed/(mm/s)
−5 ~ +3.5	8	600	14

Figure 8 The difference in building height of a thin-walled part can be compensated automatically in several layers



Notes: (a) The relationship between the laser defocusing distance and height of single tracks; (b) the surface unevenness of thin-walled part

According to the relationship between the laser spot size and powder convergent diameter as seen from Table V and Figure 6, the laser spot size was approximately equal to the powder convergent diameter when the laser defocusing distance was up to about ±2.5 mm, and that's to say, almost all powder was injected into molten pool and the building height was the largest. When the absolute value of laser defocusing distance was larger than 2.5 mm, the laser spot size was bigger than powder convergent diameter. Although the molten pool produced by laser beam became bigger, the powder injected into molten pool was constant, so the height decreased in this condition. Conversely, when the absolute value of laser defocusing distance was less than 2.5 mm, the powder convergent diameter was larger than the laser spot size, and with the decrease of laser defocusing distance, the laser spot size became smaller. The small laser spot size created small molten pool, which made powder amount injected into molten pool reduce and the building height decrease.

Figure 8(b) shows the schematic diagram of the surface unevenness for interpreting the automatic compensation of the height variation when fabricating a multi-layer thin-walled part and obtaining the reasonable laser defocusing distances with the existing self-regulation effect.

Supposing the laser defocusing distances were set to Z_2 or Z_2' which was the target surface position, then Z_1 or Z_1' was the convex position and Z_3 or Z_3' the concave position, respectively.

The laser defocusing distance was adjusted at the range from −2.5 to −5 mm or +0.5 to +2.5 mm, and there was already a slight height difference on the surface of a thin-walled part. Figure 7(a) shows that the track height at convex position (Z_1 or Z_1') was smaller than that of target position (Z_2 or Z_2'), so the deposition rate would be lower in the next deposition. Consequently, the building height at convex position decreased gradually. Similarly, the building height at concave position (Z_3 or Z_3') increased gradually. So the building height difference was compensated automatically, and thus, a so-called self-regulation effect was achieved. On the contrary, the slight difference in building height could not be compensated when the laser defocusing distances were located in other regions, as shown in Figure 7. So, the laser defocusing range between −2.5 ~ −5 mm and +0.5 ~ +2.5 mm both were called self-regulation interval.

3.3 Thin wall fabricated using self-regulation interval splicing by variable laser spot process

The splicing of the self-regulation interval was put forward for achieving the continuous sizes of the cladding layers and taking full advantage of the self-regulation effect. Because the laser spot sizes were equal with the laser defocusing distance of ±2.5 mm as seen in Table V, the position of −2.5 mm was abandoned. The self-regulation intervals of 0.5 ~ 2.5 mm and −3 ~ −5 mm were spliced to fabricate the thin-walled part. The adopted laser defocusing distances, corresponding process parameters and section sizes, are shown in Table VIII. The single-track height of 0.48 mm and the powder mass flow rate of 8 g/min were kept constant during the experiment.

The *z*-axis increment was fixed to 2/3 h which was 0.32 mm under different laser defocusing distances. The thin-walled sample was built using variable laser spot process layer by layer.

Table VIII The section sizes and process parameters with different laser defocusing distances

Laser defocusing distance/(mm)	Laser power/(W)	Scanning speed/(mm/s)	Width/ (mm)	Height/ (mm)
0.5	400	10	1.18	0.47
1	600	14	1.36	0.47
2	800	15	1.46	0.49
2.5	1,000	14	1.55	0.49
−3	1,000	15	1.53	0.46
−4	900	11	1.90	0.47
−5	1,000	10	2.43	0.49

The layer number of the thin-walled sample was 100 and the total building height was 30 mm. The thin-walled sample fabricated is shown in Figure 9.

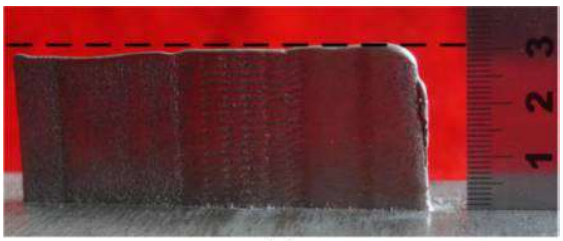
As seen from Figure 9, the forming quality of the thin-walled sample was good and its surface was relatively smooth. The width range of the sample was varying from about 1.0 to 3.0 mm. However, the total building height was not consistent. It showed that the growth rate of the large ratio of width to height position was more than the small ratio.

The reason was that laser intensity distributions were different at varying laser spot sizes. Here, α was used for defining the section order of laser intensity distribution. For example, Figure 10 shows that α changed along with the different laser intensity distributions.

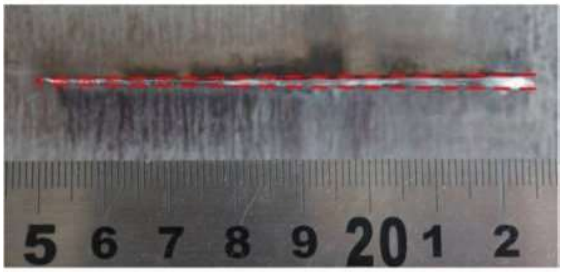
Figure 11 is the geometry morphology of the cladding layer section, whose contour curve equation is depicted in equation (2):

$$f(x) = -ax^{\alpha} + h \tag{2}$$

Figure 9 A thin-walled sample fabricated by self-regulation interval splicing



(a)



(b)

Notes: (a) The front view; (b) the top view

Figure 10 Laser intensity distribution with different laser defocusing states

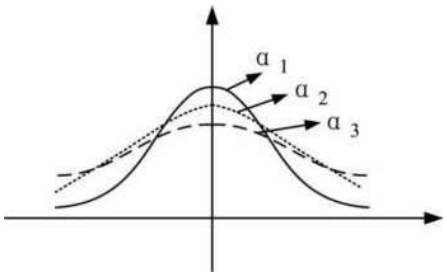
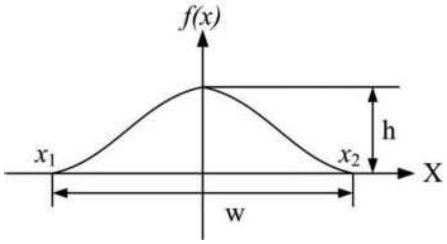


Figure 11 Section geometry morphology of cladding layer



where h was the height of single track, a was the undetermined coefficient.

In equation (2), there were at least two real roots x_1 and x_2 by solving zero point, as shown in equation (3). The distance between zero x_1 and x_2 was the width of single track, and then the coefficient a could be solved by substituting equation (3) into equation (4). The contour curve equation of cladding layer section was then acquired, as shown in equation (5):

$$f(x)=0 \Rightarrow x_{1,2}=\pm\sqrt{\frac{h}{a}} \tag{3}$$

$$w = 2\sqrt{\frac{h}{a}} \Rightarrow \mathrm{a} = \frac{2^{\alpha} \times h}{w^{\alpha}} \tag{4}$$

$$f(x) = -\frac{2^{\alpha} \times h}{w^{\alpha}} \times x^{\alpha} + h \tag{5}$$

The necessary condition of top smoothness of cladding layer was that the z-axis increment ΔZ was equal to the real growth of cladding layer, that is to say, the area $2S_1$ should be equal to $2S_2$, as shown in Figure 12. Because the area was symmetrical, the area S_1 was equal to S_2.

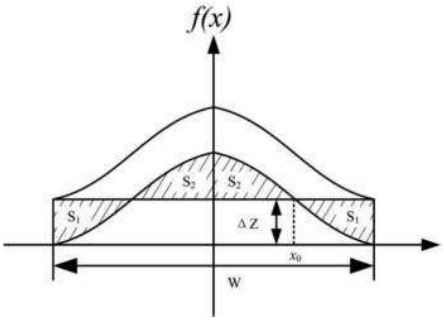
From Figure 12, the areas S_1 and S_2 were calculated as followed:

$$S_1 = \left(\frac{w}{2} - x_0\right) \times \Delta Z - \int_{x_0}^{\frac{w}{2}} f(x)dx \tag{6}$$

$$S_2 = \int_0^{\frac{w}{2}} f(x)dx - x_0 \times \Delta Z - \int_{x_0}^{\frac{w}{2}} f(x)dx \tag{7}$$

Downloaded by 121.228.30.1 At 15:16 08 February 2018 (PT)

Figure 12 Accumulation section morphology under ideal state



$$S_1 = S_2 \Rightarrow \int_0^{\frac{w}{2}} f(x)dx = \frac{w}{2} \times \Delta Z \tag{8}$$

Substituting equation (5) into equation (8), the z-axis increment ΔZ was obtained:

$$\Delta Z = \frac{\alpha}{\alpha + 1} \times h \tag{9}$$

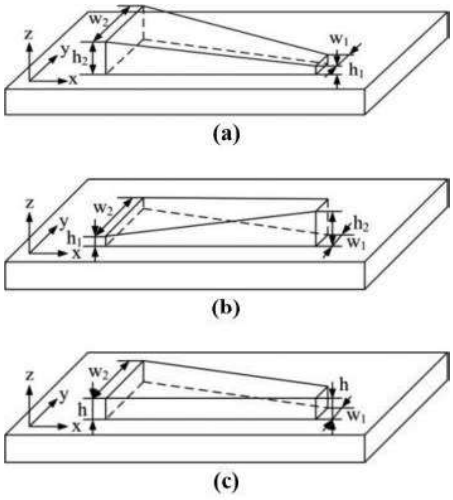
As seen from equation (9), the z-axis increment was only related to the curve order α when the height of cladding layer was constant.

Equation (2) shows that the bigger the curve order α was, the smoother the cladding layer surface was. Namely, the curve order α was representative of smooth level of the cladding layer surface. At the same time, the bigger ratio of width to height was, the smoother the cladding layer surface was. The curve order α was proportional to the ratio of width to height. Therefore, the bigger ratio of width to height was, the more the curve order α was. So, the bigger the z-axis increment was, the bigger the ratio was when varying the laser spot. However, the z-axis increment was constant during deposition, and a uniform z-axis increment would cause a very close distance between the nozzle and molten pool in large ratio position, as seen from Figure 9. In addition, the smaller the distance was, the bigger the powder concentration was. The growth rate of cladding layer in the large ratio position was more than the small ratio position. The building heights of cladding layers were not consistent and the whole top surface was also not smooth. What is worse, the cladding layers would crack and lead to cease with the increase of cladding layer number.

3.4 Thin wall fabricated using stepped single-track method based on self-regulation interval splicing by variable laser spot process

A stepped single-track method was designed for solving the problem mentioned in 3.3 which was the inconsistent building height because of the different ratios of width to height. The growth rate of the large ratio position was more than the small ratio position under a uniform Z-increment, and the actual section is shown in Figure 13(a) ($w_2 > w_1$; $h_2 > h_1$). Adjusting the process parameters to make the growth rate of the large ratio position be less than the small ratio position, as shown in Figure 13(b) ($w_2 > w_1$; $h_2 < h_1$), namely, a so-called stepped single-track method was designed. Sequentially, a uniform building height of cladding layers could be acquired, and the ideal section is shown in Figure 13(c) ($w_2 > w_1$; $h_2 = h_1$).

Figure 13 Longitudinal section geometry morphology of cladding layer

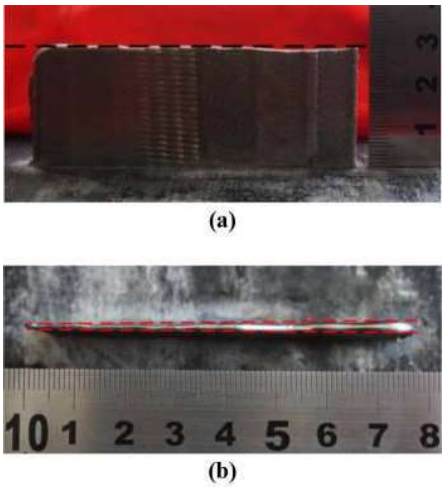


Notes: (a) Actual section; (b) designed section; (c) ideal section

Table IX Section sizes of cladding layers with different laser defocusing distances

Defocus distance/(mm)	Power/(W)	Scanning speed/(mm/s)	Width/(mm)	Order	Height/(mm)
0.5	300	10	1.18	2.5	0.47
1	600	15	1.36	2.5	0.47
2	1,000	15	1.71	2.5	0.46
2.5	800	15	2.25	5.5	0.40
−3	1,000	15	1.53	2.5	0.46
−4	600	10	1.78	3.5	0.44
−5	600	5	2.58	7	0.39

Figure 14 A thin-walled sample using stepped single-track by self-regulation interval splicing



Notes: (a) The front view; (b) the top view

Downloaded by 121.228.30.1 At 15:16 08 February 2018 (PT)

To get the height values designed of cladding layer with different laser defocusing distances, first of all, the index function fitting way was adopted to acquire the contour curve equations of cladding layer section under the same height of single track, and then the curve order was caught according to the equations. Second, the orders were substituted into equation (9) with the uniform z-axis increment of 0.32 mm. Finally, the heights with different laser defocusing distances could be calculated, as shown in Table IX.

The thin-walled sample was built using stepped single-track method by variable laser spot process with the process parameters listed in Table IX. The layer number of the thin-walled sample was 100, and the total building height was about 30 mm. The thin-walled sample fabricated is shown in Figure 14.

As it is observed from Figure 14, the forming quality of the thin-walled part was good and its surface was also smooth. The width range was also about from 1.0 to 3.0 mm, which could achieve the requirement set in advance.

4. Applications

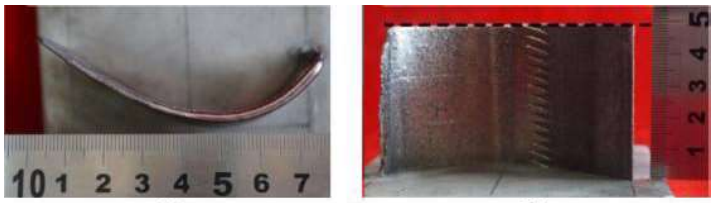
4.1 Thin-walled blade fabricated using stepped single-track method

To further verify the process feasibility, a thin-walled blade was fabricated using stepped single-track method layer by layer with the process parameters listed in Table IX. The layer number of the thin-walled blade was 150, and the total building height was about 49 mm. The fabricated thin-walled blade is shown in Figure 15. The forming quality of the thin-walled blade was good and its surface was smooth. The width of the sample was also gradually increased from 1.0 to 3.0 mm.

4.2 Microstructural characteristics

The microstructure of the component determined the mechanical properties and performance under variable laser spot process. The optical examination was carried out on the thin-walled blade with the different laser defocusing distances

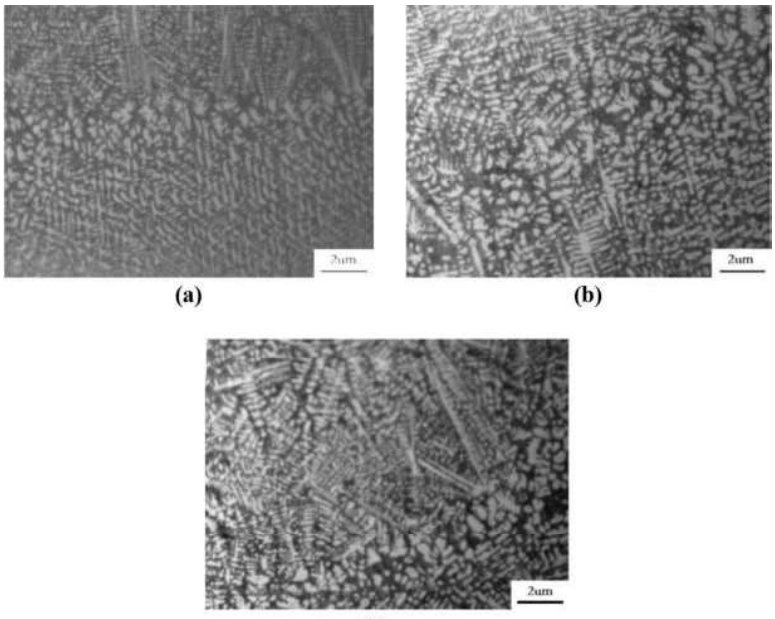
Figure 15 A thin-walled blade using stepped single-track



(a) (b)

Notes: (a) The front view; (b) the top view

Figure 16 Microstructure of the thin-walled blade with Z = 0.5 mm examined at different positions



(a) (b)

(c)

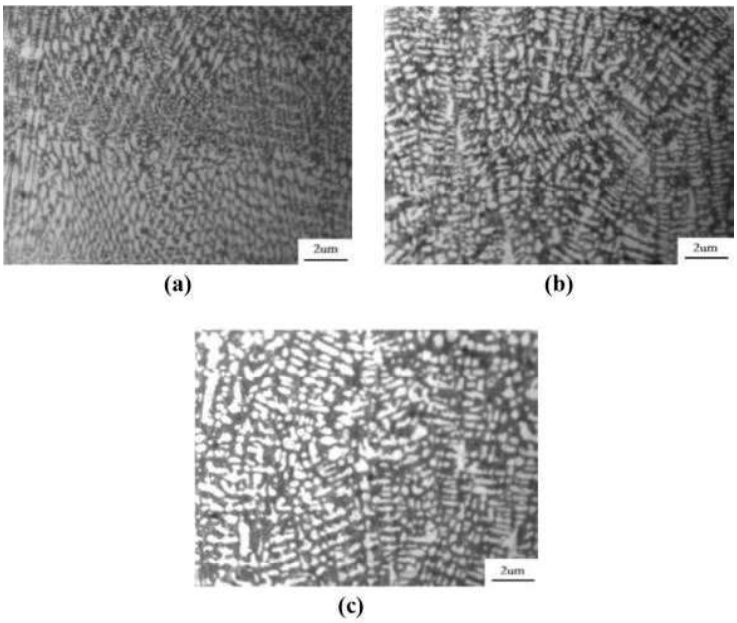
Notes: (a) Bottom; (b) middle; (c) top

Downloaded by 121.228.30.1 At 15:16 08 February 2018 (PT)

of 0.5, 2.5 and −5 mm. The microstructures were examined in the region of the bottom, middle and top, respectively, as shown in Figures 16, 17 and 18.

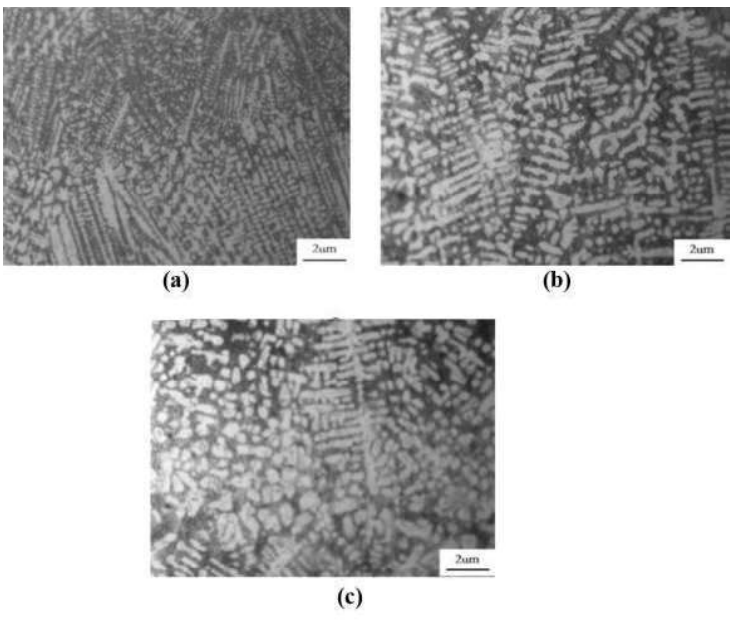
As can be seen from Figures 16, 17 and 18, no pores and microcracks were observed in the section. It could be identified that the microstructures showed cellular grains. The differences were that the microstructures became coarser with the increasing absolute value of laser defocusing distance. Because the larger laser defocusing distance produced bigger molten pool, the width of molten pool became bigger, the solidification time of molten pool increased, the cooling rate decreased, the temperature gradient reduced, the nucleation rate decreased and the cellular grains were also larger.

Figure 17 Microstructure of the thin-walled blade with Z = 2.5 mm examined at different positions



Notes: (a) Bottom; (b) middle; (c) top

Figure 18 Microstructure of the thin-walled blade with Z = −5 mm examined at different positions



Notes: (a) Bottom; (b) middle; (c) top

Downloaded by 121.228.30.1 At 15:16 08 February 2018 (PT)

5. Conclusions

A new varying laser spot process was put forward to fabricate single track with unequal width by one scanning rather than multi-track overlapping based on the way of inside-beam powder feeding method, and the thin-walled parts were fabricated layer by layer using LDMD technology. The unequal-width thin-walled parts with good forming quality was fabricated successfully. Some of conclusions were summarized:

- A uniform height of single track with unequal width by controlling scanning speed and laser power was obtained with varying laser spot and sufficient powder mass flow rate.
- The self-regulation effect worked within the laser defocusing range from −2.5 to −5 mm and +0.5 to +2.5 mm. The thin-walled parts were fabricated layer by layer by splicing the self- regulation interval and its forming quality was improved in a certain degree.
- The growth rate of cladding layers was not consistent under a uniform height of single track, and the growth rate of the large ratio of width to height position was more than that of the small ratio position.
- The theoretical model, among layer thickness of *z*-axis, height of single track and the section curve order of cladding layer, was established. The thin-walled parts with smooth surface and good forming quality were fabricated using stepped single-track method by splicing self-regulation interval with continuously variable width from 1 to 3 mm.

References

Cao, J., Liu, F.C., Lin, X., Huang, C.P., Chen, J. and Huang, W.D. (2013), "Effect of overlap rate on recrystallization behaviors of laser solid formed inconel 718 superalloy", *Optics & Laser Technology*, Vol. 45 No. 2, pp. 228-235.

Dinda, G.P., Dasgupta, A.K. and Mazumder, J. (2009), "Laser aided direct metal deposition of inconel 625 superalloy: microstructural evolution and thermal stability", *Materials Science and Engineering A*, Vol. 509 Nos 1/2, pp. 98-104.

Dutta, B., Singh, V., Natu, H., Choi, J. and Mazumder, J. (2009), "Direct metal deposition", *Advanced Materials & Processes*, Vol. 167 No. 3, pp. 29-31.

Gu, D.D., Meiners, W., Wissenbach, K. and Poprawe, R. (2012), "Laser additive manufacturing of metallic components: materials, processes and mechanisms", *International Materials Reviews*, Vol. 57 No. 3, pp. 133-164.

Li, D.C., He, J.K., Tian, X.Y., Liu, Y.X., Zhang, A.F., Lian, Q., Jin, Z.M. and Lu, B.H. (2013), "Additive manufacturing: integrated fabrication of macro/microstructures", *Journal of Mechanical Engineering*, Vol. 49 No. 6, pp. 129-135.

Li, P., Ji, S.Q., Zeng, X.Y., Hu, Q.W. and Xiong, W.H. (2007), "Direct laser fabrication of thin-walled metal parts under open-loop control", *International Journal of Machine Tools Manufacture*, Vol. 47 No. 6, pp. 996-1002.

Mazumder, J., Dutta, D., Kikuchi, N. and Ghosh, A. (2000), "Closed loop direct metal deposition: art to part", *Optics and Lasers in Engineering*, Vol. 34 Nos 4/6, pp. 397-414.

Peis REIS LASERTEC. (2011), "A variable focal length nozzle", available at: www.reislasertec.de/cn/produkte/laser-processing-optics/powder-optics/00032

Pi, G., Zhang, A.F., Zhu, G.X., Li, D.C. and Lu, B.H. (2011), "Research on the forming process of three-dimensional metal parts fabricated by laser direct metal forming", *The International Journal of Advanced Manufacturing Technology*, Vol. 57 Nos 9/12, pp. 841-847.

Pinkerton, A.J. and Li, L. (2004), "The significance of deposition point standoff variations in multiple-layer coaxial laser cladding (coaxial cladding standoff effects)", *International Journal of Machine Tools Manufacture*, Vol. 44 No. 6, pp. 573-584.

Shi, S.H., Fu, G.Y., Wang, A.J., Zhang, Y., Zhu, P.F. and Hu, J. (2006), "Laser forming manufacturing process and nozzle of inside-laser powder feeding", Chinese Patent, CN200610116413.

Wang, H.M. (2014), "Materials' fundamental issues of laser additive manufacturing for high-performance large metallic components", *Acta Aeroautica et Astronautica Sinica*, Vol. 35 No. 10, pp. 2690-2698.

Wu, X. (2007), "A review of laser fabrication of metallic engineering components and of materials", *Materials Science and Technology*, Vol. 23 No. 6, pp. 631-640.

Zhu, G.X. (2011), *Laser metal direct forming process of hollow turbine blades*, Xi'an Jiaotong University, Xi'an, p. 61.

Corresponding authors

Gangxian Zhu can be contacted at: gxzhu@suda.edu.cn and **Tuo Shi** can be contacted at: tuo.shi@qq.com

For instructions on how to order reprints of this article, please visit our website:
www.emeraldgrouppublishing.com/licensing/reprints.htm
Or contact us for further details: **permissions@emeraldinsight.com**

Downloaded by 121.228.30.1 At 15:16 08 February 2018 (PT)